TWO TOMATO ENDOGLUCANASES HAVE A FUNCTION DURING SYNCYTIUM DEVELOPMENT

MAŁGORZATA LICHOCKA, WŁADYSŁAW GOLINOWSKI

Department of Botany, Faculty of Agriculture and Biology,
Warsaw Agricultural University
Nowoursynowska 159, Building 37, 02-776 Warszawa, Poland
e-mail: malgorzata.lichocka@googlemail.com

(Received: November 30, 2006. Accepted: March 6, 2007)

ABSTRACT

Globodera rostochiensis, as well as other cyst nematodes, induces formation of a multinucleate feeding site, called syncytium, in host roots. In tomato roots infected with a potato cyst nematode, the syncytium is initiated in the cortex or pericycle. Progressive cell wall dissolution and subsequent fusion of protoplasts of newly incorporated cells lead to syncytium formation. Expansion and development of a syncytium strongly depends on modifications of a cell wall, including its degradation, elongation, thickening, and formation of ingrowths within it in close contact with tracheary elements. Recent reports have demonstrated that during formation of syncytium, numerous genes of plant origin, coding for cell wall-modifying enzymes are up-regulated. In this research, we studied a detailed distribution and function of two tomato β-1,4-endoglucanases in developing feeding sites induced by *G. rostochiensis*. In situ localization of tomato *LeCel7* and *LeCel8* transcripts and proteins demonstrated that these enzymes were specifically up-regulated within syncytium and in the cells adjacent to the syncytium. In non-infected roots an expression of *LeCel7* and *LeCel8* was observed in the root cap and lateral root primordia. Our data confirm that cell wall-modifying enzymes of plant origin have a role in a modification of cell wall within syncytia, and demonstrate that plant endoglucanases are involved in syncytia formation.

KEY WORDS: potato cyst nematode, syncytium, 1,4-β-endoglucanases, cell wall modification.

INTRODUCTION

Potato cyst nematodes (*Globodera rostochiensis*) are obligate, sedentary endoparasites, which after invasion of host-plant roots induce changes in an expression of numerous plant genes during the formation of feeding cells (Gheysen and Fenoll 2002). To complete their life cycle, the sedentary nematodes depend entirely on the successful induction and maintenance of specialized feeding cells. Feeding cells formed by the cyst nematodes, called syncytia, are multinucleate structures that develop from a single cell, called the initial syncytial cell (ISC). The infective juvenile stage of a potato cyst nematode selects a competent root cell from the cortex or pericycle (Jones and Northcote 1972; Goverse et al. 2000). Subsequent incorporation of cells adjacent to ISC via extensive cell wall dissolution and protoplast fusion leads to the formation of a syncytium (Golinowski et al. 1997). Cells that are incorporated into syncytia undergo significant modifications, in the effect of which they are no more separate individuals, but become highly hypertrophied syncytial elements with dense cytoplasm. Features of a syncytium protoplast include the absence of the central vacuole; proliferation of the rough and smooth ER, ribosomes, mitochondria and plastids; the formation of numerous lipid bodies (Golinowski et al. 1997); and nuclei enlargement by DNA endoreduplication (Endo 1971; Niebel et al. 1996). In syncytia induced by cyst nematodes, cell wall ingrowths are formed in syncytial elements in close contact with xylem elements. A syncytium has also features of transfer cells because it facilitates transfer of nutrients from a host plant to the nematode developing within the plant (Jones and Northcote 1972). Intensive demand of nematodes for nutrient stimulates a specific manner of syncytium expansion. The syncytium expands mostly longitudinally along the length of the vascular cylinder by incorporation of the cells adjacent to the xylem and phloem elements.

The structure of syncytia suggests that extensive cell wall modifications (i.e., thickening, ingrowth, disassembly and dissolution) are required for the formation of feeding structures. These changes are mediated by the activity of both cell wall-biosynthetic and cell wall-degrading enzymes. It is well known that during migration in root tissues infective larvae of cyst nematodes secrete numerous hydrolytic enzymes or modifying proteins for digesting cell wall polymers such as endo-β-1,4-glucanases (Smant et al.

1998; Gao et al. 2004), pectate lyases (Popeijus et al. 2000), and expansins (Qin et al. 2004). But the expression of these proteins was no more detectable, since the larvae selected the initial syncytial cell and became sedentary. Recent studies have demonstrated that cell wall-degrading enzymes in developing syncytia were of plant origin. Goellner et al. (2001) showed a local up-regulation of five tobacco endo-β-1,4-endoglucanases genes in tobacco roots infected with tobacco cyst nematodes. Karczmarek (2006) demonstrated that in tomato roots infected with *G. rostochiensis* only two endo-β-1,4-endoglucanases genes *LeCel7* and *LeCel8* were up-regulated in the young syncytia. Plant endo-β-1,4-endoglucanases (EGases) catalyse the breakdown of β-1,4 glucosidic linkages. These enzymes belong to glycosyl hydrolase family 9 (Henrissat 1991) and their substrates probably include xyloglucan, integral and peripheral regions of non-crystalline cellulose and possibly glucomannan (Brummell and Harpster 2001). EGases have been shown to be expressed during fruit ripening, senescence, in elongating and expanding cells, which suggests a role in plant development (Lashbrook et al. 1994; del Campillo and Bennett 1996; Catala et al. 1997; Catala et al. 2000).

In this article, we characterized a spatial and temporal expression of *LeCel7* and *LeCel8* within tomato root cells modified by potato cyst nematodes. We monitored these changes at the transcriptional and translational levels. In the infected roots, transcripts and proteins of both enzymes were present in or very close to the developing syncytia. Expression of both genes were strictly correlated with the development of the syncytium. More detailed studies with the use of polyclonal antibodies revealed a detailed localization of these enzymes at a subcellular level. This is the first immunolocalization of plant endoglucanases at subcellular level in plant roots infected with plant parasitic nematode. The obtained results suggest that these two enzymes: LeCel7 and LeCel8, play a role in cell wall metabolism in expanding syncytium.

MATERIALS AND METHODS

Plant material and nematode inoculation

Seeds of tomato (*Lycopersicon esculentum*) cv. Money Maker were surface sterilized with solution of commercial bleach, containing 1.25% sodium hypochlorite (NaOCl) and detergents, for 10 min. Seeds were washed with the sterile distilled water 3 times for 10 min and transferred onto Petri dishes containing 1.5% water agar and left in the darkness at 20°C for germination. Seedlings were transferred aseptically into 9-cm Petri dishes containing Gamborg B5 agar medium. Tomato plants were grown in sealed dishes for 10 days at 20°C under 16-h photoperiod and 110 $\mu E\ m^{-2}s^{-1}$.

Tomato roots were inoculated with second-stage infective juveniles (J2) of the potato cyst nematode *Globodera rostochiensis*, pathotype Ro1, Mirenbos. Larvae were stimulated to hatching by incubation of cyst in the potato root exudates. A freshly hatched juveniles were surface sterilized in 0.025% $HgCl_2$ for 2 min and extensively washed in several changes of sterile distilled water. Water drops, each containing approximately 20 individual J2/per root tip, were transferred to 10 days-old tomato plants. After inoculation plants were kept in the darkness at 20°C. Each day, inoculated plants were screened for the presence of J2s inside the roots. The developmental stages of syncytium were counted in days post infection, since first sign of the presence of J2s inside the roots were observed.

For microscopic examinations, the inoculated roots were screened for the presence of J2s inside the roots each day after inoculation. Root fragments with juveniles were collected at 1, 2, 3, 5, 14 days post root infection. Collected material was pre-fixed for 2-3 h in a mixture of paraformaldehyde (2%) and glutaraldehyde (2%) in 0.5 M sodium cacodylate buffer at pH 7.2-7.3 and post-fixed for 2 h in 1% osmium tetroxide at 4°C. Samples were dehydrated in ethanol and propylene oxide and embedded in epoxy resin (Fluka) as described by Golinowski et al. (1996). Semi-thin (3 µm) and ultra-thin (70 to 80 nm) sections were cut using Leica RM 2165 microtome and Leica Ultracut UCT ultramicrotome. Ultra-thin sections were collected on copper grids and stained for 4 min with saturated 50% ethanol solution of uranyl acetate, followed by 6 min of staining with an aqueous solution of lead citrate. The sections were examined using Phillips Morgagni transmission electron microscope equipped with the digital camera (Morada).

Plant material for in situ examination and immunolocalization

Samples containing segments of the roots with syncytia were collected at 3, 7, 10, 14 days post infection. They were fixed in 2% paraformaldehyde/2% glutaraldehyde and 4% paraformaldehyde/1% glutaraldehyde in 50 mM PBS buffer (pH 6.9) for 2 h at room temperature. Fixed samples were washed 4 times for 20 min in the same buffer; they were dehydrated and embedded in butyl-methyl-methacrylate (BMM) resin as described by De Almeida Engler et al. (2001). Samples for immunogold labeling after dehydration in series of ethanol solutions were embedded in London Resin White. Material embedded in LR White was cut into ultra-thin sections using Leica Ultracut UCT ultramicrotome. Material embedded in BMM was cut into semi-thin sections (3 µm) using Leica RM2165 microtome. For in situ analysis and immunolocalization, slides with sections were incubated in 100% acetone for 15 min to remove BMM resin.

Digoxygenine (DIG)-labeled ss-cDNA and ds-cDNA probes

Digoxygenine (DIG)-labeled ss-cDNA probes for *LeCel7* and *LeCel8* were prepared in two successive amplification reaction using primer pairs (Table 1). In 1st reaction – RT PCR, ds-cDNA fragments were generated with one of the primer pairs, using total RNA isolated from tomato roots (Rneasy Plant Mini Kit, Qiagen) containing syncytia, as a template. In a 2nd reaction, a PCR DIG Probe Synthesis Kit (Roche) was used to synthesise antisense or sense ss-cDNA probes with 1 µl of the 1st RT PCR product as a template and a single primer. ds-cDNA DIG-labeled pro-

TABLE 1. Primer pairs used for ss-cDNA and ds-cDNA probe synthesis and for in situ RT PCR.

Primer pair	Primer forward	Primer rewers
LeCel7	5'-gattcattcaaacaaagagcggaag	5'-gcattgccaaagaaggtaaagatg
LeCel8	5'-tggtcacagcggttacaatc	5'-cgattgcaggtgaagcagtgtg

bes were generated by adding one of the primer pairs and 1 µl of the 1st RT PCR product into PCR mixture. Reactions were performed on a MJ Research PTC-100 thermal cycler using the following PCR profile: 1 cycle at 95˚C for 5 min followed by 35 cycles of 30 s at 95˚C, 30 s at 54˚C, and 50 s at 72˚C, followed by 7 min at 72˚C. The probes were purified from unincorporated nucleotides with a Mini Quick Spin DNA Columns (Roche). Products were analysed on 1.5% agarose gel.

In situ hybridization and in situ RT PCR followed by hybridyzation

For in situ hybridization, rehydrated tissue sections were pretreated with Proteinase K (2 µg/ml) in 0.05 M Tris pH 7.5 at 37˚C for 20 min. After washing, sections were dehydrated in a graded ethanol series, and air dried. Hybridization solution (50% formamide, 10% dextran sulphate, 250 ng/ml tRNA, 100 µg/ml Poly (A), 0.3 M NaCl, 0.01 M Tris (pH 7.5), 1 mM EDTA, 1×Denhard's solution, 0.01 DTT) was supplemented with 2 µg/ml DIG-labeled ss-cDNA antisense or sense probe. Slides were sealed and kept overnight at 42˚C. Afterwards section were washed in 2×SSC (saline-sodium citrate buffer, pH 7.2) for 15 min at 42˚C, once in 1×SSC at 42˚C, followed by 3 washes with sterile distilled water for 1 min. Hybridized DIG-labeled transcripts were immunolocalized with Fluorescent Antibody Enhancer for DIG Detection (Roche). Slides were air dried and mounted with Immuno-Fluore Mounting Medium (ICN). Slides were viewed using an AX70 Provis microscope (Olympus, Japan) equipped with a U-M61002 fluorescence filter set.

For in situ RT PCR slides were rehydrated, digested with Proteinase K and dehydrated again as described above. Pre-treated slides were treated with RNase free DNase I solution (1 kU/ml Dnase I, (Roche), 100 mM sodium acetate buffer pH 5.5, 5 mM $MgSO_4$) overnight at 36˚C. In situ RT PCR were performed with a Titan One Tube RT PCR Kit (Roche) supplemented with primer pairs *LeCel7* and *LeCel8* (600 nM each) (Table 1) and 1×Self-Seal Reagent (MJ Research). The RT PCR cycles were as follows: reverse transcription for 45 min at 50˚C, followed by 45 cycles of 45 s at 94˚C, 30 s at 54˚C, 1min at 68˚C. Slides were kept for 10 min at 68˚C, for 1 min at 92˚C and stored at 4˚C. Before hybridization, slides were washed with 2×SSC for 5 min. Hybiridization solution (described above) was supplemented with 1 µg/ml of DIG labeled ds-cDNA probe and dispensed onto slides containing sections. Slides were sealed and kept for 10 min at 85˚C for denaturation of amplified cDNA and DIG-labeled ds-cDNA probes. Hybridization, posthybridization treatment and immunodetection were performed as described above.

Antibodies production

The pBAD/Thio-TOPO expression system (Invitrogen) was used for the production of LeCel7 and LeCel8 recombinant protein for immunization of chicken (Laboratory of Nematology, Wageningen). Recombinant proteins consisted of 70 amino acid fragment (~7 kDa) of LeCel7 and LeCel8, thioredoxin (11,2 kDa) and V5/His peptide. The amino acid sequence of LeCel7 recognized by IgY antibodies: 237 LLR ATNDISYLNL INTLGANDVP DLFSWDNKYA GAHVLMSRRS VVGNDNRFDS FKQRAEDFVC KVLPNSPY 308. Antibodies against LeCel8 recognised 70 amino acid fragment of a putative cellulose binding domain at the C terminus: 543 alngkty yrysavvtnk sgktvknlkl sivklygplw gltkygnsfi fpawlnslpa gkslefvyih tas 614. IgY antibodies were precipitated from the yolk by PEG 6000 and affinity-purified on a HiTrap IgY column (Amersham/Pharmacia). Antibodies against LeCel7 were additionally raised in rabbit. The amino acid sequence of the peptide antigen PNQNDFFPDERTDYS was combined with the KLH. The antigen-KLH complex was injected into a rabbit (Genosys, Sigma). Obtained antiserum was purified with the Protein A Antibody Purification Kit (Sigma).

Immunolocalization for light and electron microscopy

Sections for light microscopy observations, after resin removal with acetone, were incubated in a blocking solution (5% non-fat dried milk in 0.01 M PBS (150 mM NaCl, 2 µM KH_2PO_4, 8 µM Na_2HPO_4 pH 7.3) for 1 h at room temperature. Afterwards sections were incubated in the primary antibody solution (IgY anti-LeCel7 and anti-LeCel8 diluted 1:10 or 1:20 in PBS, IgG anti-LeCel7 1:10) for 2 h at room temperature. As a negative control, primary antibodies were replaced by the pre-immune serum from chicken or rabbit. After washing in PBST (0.05% Tween 20 in PBS) sections were incubated for 1 h with the secondary antibodies: anti IgY conjugated to the Alexa Flour 488 (Molecular Probes), anti IgG conjugated to the fluorescein isothiocyanate (FITC) (Sigma). The sections were washed as described above and stained with 1 µg/ml DAPI for 5 min, with 0.01% toluidine blue for 5 min. Slides were examined as described above for in situ analysis.

Material embedded in LR White resin was cut into ultrathin sections and mounted onto the nickel grids, previously coated with formvar. Grids were incubated on drops of following solutions: the blocking solution, the primary antibodies and the washing solution as described above. After washing, sections were incubated with the secondary antibodies anti IgY and IgG, conjugated to the colloidal gold: 18 nm and 10 nm respectively in diameter. The excess of the antibodies was removed by washing in PBST. Sections were stained for 10 min in 2% water solution of uranyl acetate. Afterwards grids were intensively washed with water and air-dried. The sections were examined using Phillips Morgagni transmission electron microscope equipped with the digital camera Morada.

RESULTS

Cell wall modifications in developing syncytia

A first evidence of modifications of cell walls in the developing syncytia occurred very early, after initiation of a syncytium. After the invasion of the tomato roots, larvae of potato cyst nematode (PCN, *G. rostochiensis*) induced syncytia in the cortex (Fig. 1A) and pericycle. First openings in a cell wall, between initial syncytial cell (ISC) and adjacent cells, were formed by the gradual widening of the plasmodesmata (Fig. 1C). Protoplasts of the incorporated cells and syncytium fused (Fig. 1A). During early stage of the development of the syncytium, a column of cells was sequentially incorporated towards the vascular cylinder. At three days post infection (dpi) syncytium reached the vascular cylinder and changed the direction of its development. The syncytium continued to expand in both direc-

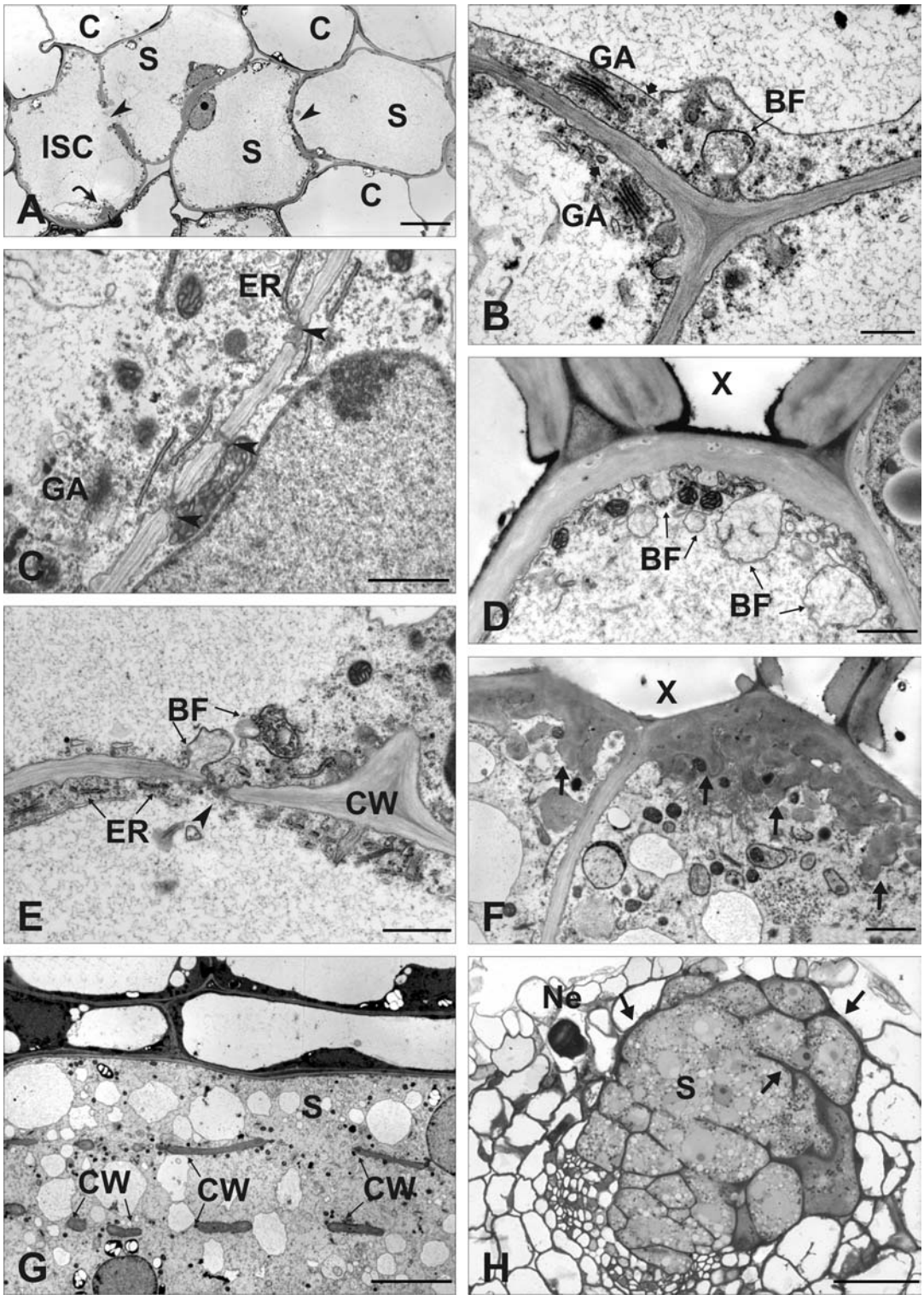

Fig. 1. Cell wall modifications in the developing syncytium.
A – syncytium (S) 1 dpi composed of cells derived from the cortex, connected by cell wall openings (arrow heads). A feeding plug (curved arrow) is visible in the initial syncytial cell (ISC). **B** – fragment of the inner syncytial wall (3 dpi), boundary formations (BF) filled with an fibrilar material. Active Golgi apparatus (GA) produce numerous Golgi vesicles (short arrows). **C** – widened plasmodesmata in syncytium 2 dpi (arrow heads). Cisternae of ER in the close vicinity to the altered plasmodesmata. **D** – numerous boundary formations (BF), filled with fibrilar material, formed by syncytial wall (5 dpi), adjoining xylem vessels (X). **E** – fragment of the inner syncytial wall (3 dpi), visible opening formation (arrow head). Cell wall stubs are associated by boundary formations (BF). **F** – cell wall ingrowths (arrows) in the 14-day-old syncytium located at the outer syncytial wall facing xylem vessels (X). **G** – cell wall fragments (CW) inside 5-day-old syncytium (S) delineate original cell boundaries. **H** – cross section through syncytium 14 dpi, close to the nematode head (Ne). Thickened syncytial wall pointed with arrows.
BF – boundary formations; C – cortex; CW – cell wall; dpi – days post induction; ER – endoplasmic reticulum; GA – Golgi apparatus; ISC – initial syncytial cell; S – syncytium; X – xylem vessels.
Bars: 50 µm in (**H**); 10 µm in (**A**), (**G**); 2 µm in (**F**); 1 µm in (**C**), (**E**), (**D**); 0.5 µm in (**B**).

tions along the vasculature. The vascular parenchyma and pericycle cells adjacent to the xylem and phloem were incorporated. The breakdown of the cell walls occurred only only after incorporation of the cell into the syncytium. The formation of openings at plasmodesmata occurred only in the 1-day-old syncytia. In the young developing syncytia, the wall openings were formed without the involvement of the plasmodesmata (Fig. 1E). Degradation started from both sides of the cell wall. In the cytoplasm, the short cisternae of rough ER were accumulated. The processes of the degradation of the cell wall were accompanied by the boundary formations (paramural bodies), filled with fibrilar material (Fig. 1E). Remnants of the inner cell wall often delineated the shape of the original cell (Fig. 1G).

The expansion of the syncytium occurs due to local degradation of a cell wall and protoplast fusion. During the early stages of the syncytium development, up to 5 dpi, new cells were intensively incorporated. After reaching the vascular cylinder, new cells were incorporated only in the distal parts of the feeding structure. The incorporated cells changed their structure and function. In the 3-day-old syncytia, the syncytial elements were slightly enlarged. About 14 dpi, the final size of the feeding structure was established (Fig. 1H). Functional plasmodesmata were not observed in the outer syncytial wall. Occasionally, a single plasmodesmata occurred between the syncytium and the sieve elements, which were filled with an electron-dense material.

Locally significant thickening of the syncytial wall was observed. During the syncytium development, the outer syncytial walls, especially those adjacent to the head of the nematode, became thickened (Fig. 1H). Thickening was also observed in the fragments of the cell wall inside the syncytia. In the young syncytia, up to 3-day-old, the outer syncytial walls and wall fragment had the smooth surface. In the-older syncytia, from 3-day-old onwards, boundary formations, containing fibrilar material, appeared at the wall fragments and inner surface of the syncytial wall. Frequently these structures were associated with thickening of the syncytial walls (Figs 1B and 1D). Numerous diotyosomes and Golgi-derived vesicles were associated with the biosynthesis of the syncytial wall. Elaborate thickening occurred in the syncytial wall adjacent to the xylem. In the 5--day-old syncytia, we observed a regularly thickened syncytial wall adjoining the xylem, associated with numerous boundary formations (Fig. 1D). From 5 dpi onwards, the thickening was less regular and the deposition of newly synthesised cell wall polymers led to the formation of a cell wall ingrowth. In the 14-day-old syncytia, the cell wall ingrowths were well developed and formed complex labyrinth (Fig. 1F). In the close vicinity, numerous mitochondria and ER were localized. Elaborate ingrowths were not always formed; however, pronounced thickening was usually observed.

In situ localization of LeCel7 and LeCel8 transcripts in PCN-infected tomato roots

In order to determine spatial and temporal expression patterns of *LeCel7* and *LeCel8*, we used two methods, namely in situ hybridization and in situ RT PCR followed by hybridization. In the non-infected roots, both endoglucanases could be detected in cytoplasm of root cap cells (Figs 2A and 2B). LeCel8 transcripts were also detected in lateral root primordia (Fig. 2C). The expression levels of *LeCel7* and *LeCel8* in the 3-day-old syncytia were similar (Figs 2D and 2E, respectively). However, the up-regulation of *LeCel7* occurred earlier, in the 1-day-old syncytia (data not shown). In the young syncytia, transcripts of *LeCel7* and *LeCel8* were regularly distributed in the syncytial cytoplasm and cells neighbouring the syncytium. The expression pattern of *LeCel7* remained at the same level in the 5--day-old (Fig. 2F) as well as in the 14-day-old syncytia (Fig. 2H). Fluorescent signal was clearly visible in the syncytial cytoplasm along the inner surface of the syncytial wall and wall fragments. In the 5-day-old syncytium, mRNA of *LeCel7* was detected in-older, cortex-derived part of the syncytium as well as in its younger part, which was localized in the vascular cylinder (Fig. 2F). However, the distribution of *LeCel8* transcripts changed during the development of the syncytium. On longitudinal sections of 5-day--old syncytium, the strongest *LeCel8* transcript signal was observed in a younger part of the feeding structure, localized in vascular cylinder (Fig. 2G). Only a weak signal was present in an-older part of the syncytium, close to the nematode head. In the 10-day-old syncytium, the strongest *LeCel8* transcript signal was detected in a distal part of the feeding structure and cells neighbouring the syncytium (Fig. 2I). As a negative control, hybridization with sense probe for *LeCel7* and *LeCel8* was performed. We did not observe any signal on sections of the syncytia (data not shown).

Immunolocalization of LeCel7 and LeCel8 in PCN-infected tomato roots

In this study, we investigated whether RNA expression correlated with protein accumulation or distribution. A localization of LeCel7 protein was performed using two types of polyclonal antibodies, against a different part of this protein and raised in chicken and rabbit. To localize LeCel8 protein, we used polyclonal antibodies raised in chicken. Immunolabeling with anti-LeCel7 and anti-LeCel8 performed on longitudinal sections of young, 3-day-old syncytia revealed a similar distribution pattern of both enzymes. The signal of LeCel7 and LeCel8 was highly syncytium-specific. In case of LeCel7, signal was observed earlier in the 1-day-old syncytia. In 3-day-old syncytia a strong signal of green fluorescence was regularly distributed in cytoplasm along syncytial walls (Fig. 3A). To the contrary, LeCel8 was detectable in the 3-day-old syncytia, but the signal was weak and not regularly distributed (Fig. 4A). The observed distribution of the LeCel7 and LeCel8 proteins within syncytia was associated with the distribution of transcripts. The labeling intensity substantially increased up to 10-day post infection. The differences in the labeling pattern within the syncytia were clearly visible for both enzymes in the 7-day-old syncytia. In the cortex-derived part of the syncytium, a signal of LeCel7 became weaker but was intensive in the distal part, composed of newly incorporated cells (Fig. 3F). In case of LeCel8 on a section of distal part of syncytium along xylem vessels, syncytial cytoplasm was also intensively labeled (Fig. 4C). In the 10-day-old syncytia, in syncytial elements derived from cortex, the LeCel8 signal became weaker (Fig. 4E). Antibodies anti-LeCel7 raised in rabbit additionally revealed the presence of this enzyme in the syncytial wall (Fig. 3G). As a negative control, the sections were incubated with pre-immune sera. Both sera did not give any unspecific signals (Fig. 3D).

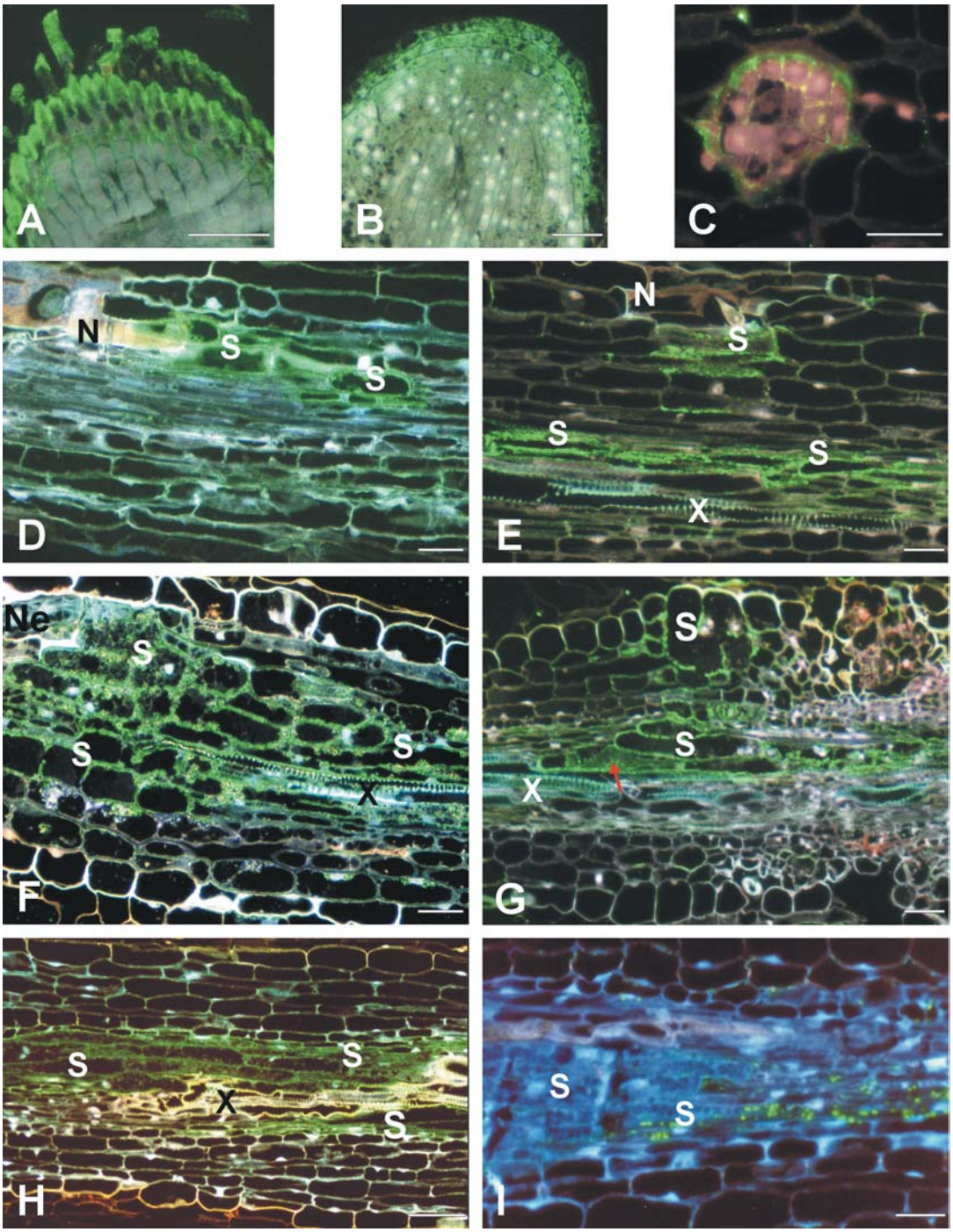

Fig. 2. In situ hybridyzation (**A-C**), (**F**), (**H**), (**I**) and in situ RT PCR followed by ISH (**D**), (**E**), (**G**) of *LeCel7* and *LeCel8* mRNA in non-infected and PCN-infected tomato roots.

In the non-infected tomato roots, mRNA of *LeCel7* (**A**) and *LeCel8* (**B**) is localized in cytoplasm of the root cap cells. (**C**) Transcripts of *LeCel8* detected in the lateral root primordia.

On longitudinal sections through a PCN-induced syncytia 3 dpi (**D**), 5 dpi (**F**), 14 dpi (**H**) transcripts of *LeCel7* regularly distributed in syncytial cytoplasm along the inner surface of the cell wall. Transcripts of *LeCel8* in 3 dpi (**E**) also detected in a thin layer of cytoplasm of the syncytial elements and cells neighbouring syncytium. (**G**) Syncytium 5 dpi – *LeCel8* mRNA level decreased in the cortex derived part of the syncytium, remains at higher levels in the distal part (red arrow). (**I**) Syncytium 10 dpi – fluorescent signal of *LeCel8* mRNA present only in the distal parts of syncytium

dpi – days post induction; N – necrosis; Ne – nematode; S – syncytium; X – xylem.

Bars: 50 µm in (**A**), (**B**), (**G**), (**H**) and 30 µm in (**C**), (**D**), (**E**), (**F**), (**I**).

In order to determine subcellular localization of LeCel7 and LeCel8, immunogold labeling was performed. The labeling pattern was similar for both enzymes and was constant during development of the syncytium. The LeCel7 and LeCel8 proteins were localised within and in close proximity to the endoplasmic reticulum (Figs 3B and 3C, and Fig. 4B). The short cisternae of rough ER were distributed along the syncytial wall. We could observe that similar ER structures in cells neighbouring syncytium were free of gold particles (Figs 3B and 4B). Locally, the proteins of LeCel7 were regularly dispersed in the syncytial cytoplasm (Fig. 3F). In case of LeCel8, intense labeling was associated with the tubular and fibrilar structures in close vicinity of the inner wall layer, but no labelling was observed in the

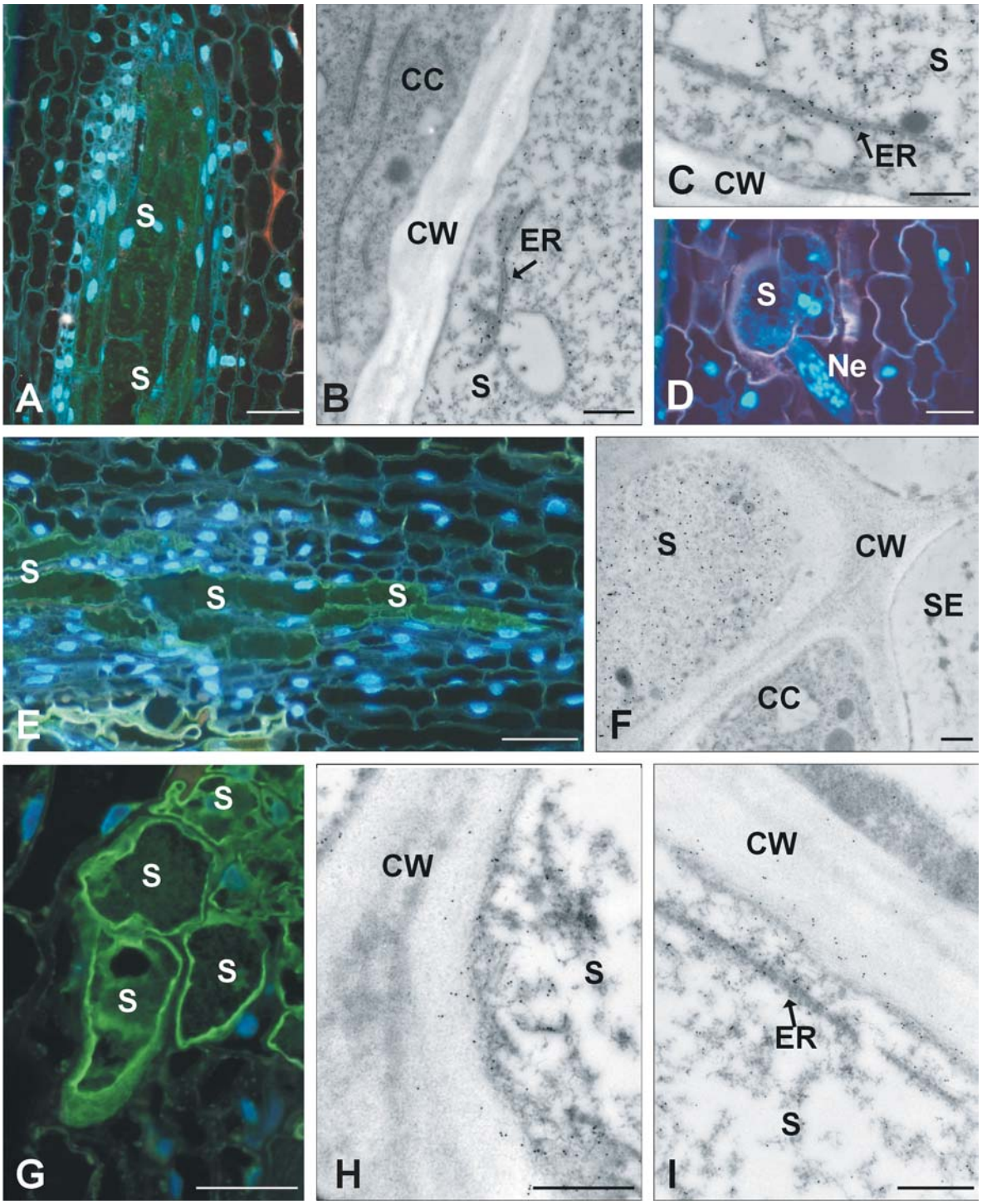

Fig. 3. Immunolocalization of LeCel7 in developing syncytium, using polyclonal IgY antibodies (**A**-**F**) and IgG (**G**-**I**).
On longitudinal semi-thin sections of syncytium 3 dpi (**A**) and 7 dpi (**E**) detection of LeCel7 with the use of IgY antibody was performed – enzyme detected only within syncytial cytoplasm (**G**) Detection of LeCel7 with the use of IgG antibodies – LeCel7 present in the syncytial wall (14 dpi) and the syncytial cytoplasm.
Immunogold labeling demonstrated presence of LeCel7 within and around ER in the developing syncytium 3 dpi (**B**), (**C**) and 7 dpi (**I**). IgY antibodies recognized LeCel7 only within cytoplasm of syncytial elements – 14 dpi (**F**). IgG antibodies demonstrated presence of LeCel7 on the inner surface of the syncytial wall – 7 dpi (**H**) and ER (**I**).
(**D**) Negative control. Sections of 3 dpi syncytium were incubated with pre-immune serum from chicken eggs.
CC – companion cell; CW – cell wall; dpi – days post induction; ER – endoplasmic reticulum; Ne – nematode; S – syncytium; SE – sieve tube.
Bars: 50 µm in (**E**); 30 µm in (**A**), (**D**), (**G**); 0.5 µm in (**B**), (**C**), (**F**), (**H**), (**I**).

syncytial wall (Figs 4D and 4F). Antibodies raised in rabbit recognised the LeCel7 protein not only in paramural cytoplasm and ER structures (Fig. 3I), but also revealed the presence of LeCel7 in close proximity to cell wall fibrils, along the inner surface of the syncytial wall (Fig. 3H).

DISCUSSION

Our data confirmed that cell wall restructuring is necessary for expansion of a syncytium, although there is still much that remains unknown. These modifications are induced by a nematode more likely by manipulation of plant

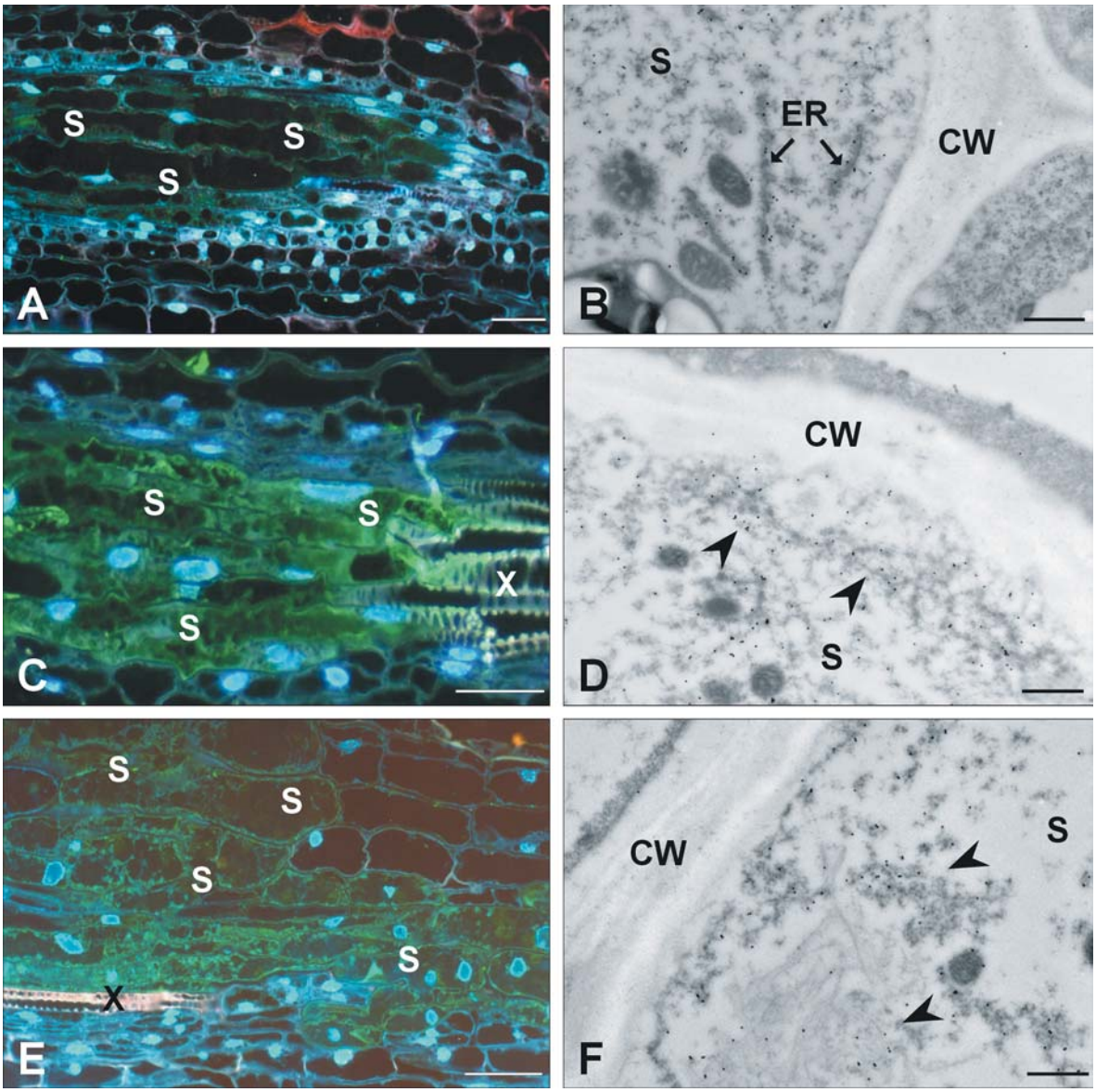

Fig. 4. Immunolocalization of LeCel8 in the developing syncytia, using polyclonal IgY antibodies.
On longitudinal sections through 3 dpi syncytia low levels of LeCel8 were detected (**A**). In-older syncytia 7 dpi (**C**) and 10 dpi (**E**) higher levels of LeCel8 were observed in the syncytial cytoplasm.
Immunogold labeling demonstrated similar distribution of LeCel8 in the syncytial cytoplasm of developing syncytia 3 dpi (**B**) 7 dpi (**D**) 14 dpi (**F**). Gold particles associated with ER tubules (**B**) and tubular and fibrilar structures (arrow heads) (**D**), (**F**), localized in the layer of cytoplasm close to the inner surface of syncytial wall.
CW – cell wall; dpi – days post induction; ER – endoplasmic reticulum; S – syncytium; X – xylem.
Bars: 50 µm in (**E**); 30 µm in (**A**), (**C**); 0.5 µm in (**B**), (**D**), (**F**).

genes at transcriptional or even translational level rather than directly by nematode secretions (reviewed by Davis et al. 2004). The process of the development of a syncytium is well documented. The complex pattern of cell wall modifications in the developing syncytium includes cell wall degradation, cell expansion, and thickening (Jones and Northcote 1972; Grundler et al. 1998). Syncytium expansion is possible only when local degradation of the cell wall occurs. Subsequent fusion of protoplast results in a multinuclear cell complex. In 2-day-old syncytia, we observed gradual widening of plasmodesmata and progressive formation of openings. Our results are in agreement with observations described by Grundler et al. (1998). They observed fully developed openings 18 h after initiation of a syncytium by *H. schachtii* in *A. thaliana* roots. Increasing volume of cytoplasm, proliferation of organelles and ribosomes, and intensive synthesis of numerous proteins led to hypertrophy of syncytial elements. We observed that process of syncytium enlargement was the most intensive from 3 to 14 days post induction. During this time, the syncytial wall underwent extension and thickening; therefore, cell wall components were intensively biosynthesised. Our results demonstrated that numerous Golgi-derived vesicles, and short cisternae of rough ER were associated with processes of rebuilding the syncytial wall. These organelles are involved in the synthesis of hemicellulose and pectin polysaccharides as well as in the glycosylation of cell wall structural proteins (Scheible and Pauly 2004). We observed that appearance of invaginations of the plasmalemma, filled with fibrilar material, was the initial step of the differentiation of a syncytial wall. These boundary formations probably contain matrix material polysacchari-

des. Rice et al. (1985) suggested that boundary formations play a role in thickening of a cell wall. Presence of boundary formation during formation of openings could be associated with removal of cell wall polysaccharides form wall stabs as well as with deposition of cell wall polysaccharides to form rounded wall stabs. We suggest that these structures may be implicated in progressive thickening of wall fragments. Deposition of a cell wall material can be locally highly elaborated. In the 10-day-old syncytia, well develop finger-like ingrowth were observed. These cell wall structures are usually typical for transfer cells, like companion-cell transfer cells (reviewed by Offler et al. 2002). Transfer cells may be involved in symbiotic associations such as mycorrhizal (Allaway et al. 1985) and rhizobium nodules (Berry et al. 1986), but also in plant-parasite interactions. Within a syncytium, cell wall ingrowths are localized against vessels and close (but not next to) the nematode head. In distal part of the-older syncytium, walls may be significantly thickened. Jones and Northcote (1972) suggested that cell wall ingrowths facilitate transfer of xylem sap into syncytium. Cell wall ingrowths are formed as a result of nematode demand for nutrients. The enlarged surface of plasmalemma intensifies short distance transport of solutes from apoplast into syncytial cytoplasm. Our observations demonstrating numerous mitochondria and ER in close vicinity of the ingrowth are in agreement with Jones and Northcote's (1972) documentation. In developing syncytium extension of syncytial wall is accompanied by its intensive thickening. Cosgrove (2005) reviewed models of the growing wall. In one of these models, enzyme-catalysed modifications of xyloglucan are considered as a key process required for wall expansion during the cell growth. Endoglucanases are one of the enzymes that probably act on xyloglucan and are up-regulated during elongation of plant cells (Wu et al. 1996; Catala et al. 1997). EGases are encoded by a large, multigene family, which in tomato consists of at least eight members. Furthermore, endoglucanases are involved in disassembly of a cell wall (Lashbrook et al. 1994), but also in the biosynthesis (Mølhøj et al. 2002).

In this paper, we studied the distribution of the *LeCel7* and *LeCel8* transcripts and proteins. So far, the activity of hydrolases within syncytia was demonstrated by the cytochemical techniques (Grundler et al. 1998). Goellner et al. (2001) observed significant up-regulation of three endoglucanases, *NtCel2*, *NtCel7*, and *NtCel8*, in a syncytium as well as in giant cells. The presence of *NtCel7* and *NtCel8* mRNA in both types of feeding sites suggested that these enzymes play a role in cell wall modifications that occur in the syncytia and giant cells. Based on their results, the authors suggested the involvement of NtCel7 and NtCel8 during the cell wall elongation and thickening but not during the cell wall dissolution, which did not occur in giant cells. Recent studies on tomato roots infected with potato cyst nematode have revealed a high expression level of two EGases, *LeCel7* and *LeCel8* (Karczmarek 2006). So far, the distribution of plant endoglucanase proteins in roots infected with plant parasitic nematode was not investigated.

Our observations of the *LeCel7* and *LeCel8* expression are consistent with Goellner's results. In situ hybridization experiments and immunolabeling showed that the expression patterns of *LeCel7* and *LeCel8* were spatially overlapping and occurred in the same syncytium region. Transcripts of both enzymes were distributed within syncytial cytoplasm and neighbouring cells. However, *LeCel7* expression was observed already in the 1-day-old syncytia, while *LeCel8* was detectable in the 3-day-old syncytia. Detection of *LeCel7* mRNA in an initial syncytial cell and during intensive incorporation of new cells suggested that this enzyme could be involved in cell wall degradation. However, further analysis with antibodies revealed that LeCel7 protein was distributed mainly along the inner surface of the syncytial wall and was associated with rough ER, fibrilar, and tubular structures localized in close vicinity of the syncytial wall. We observed a distribution pattern of the LeCel7 protein that suggests involvement of this enzyme in enlargement of syncytial elements. Our results are in agreement with previous reports. A similar subcelluar distribution of endoglucanase was observed in growing pea epicotyls stimulated with auxin 2,4-D (Bal et al. 1976). Moreover, Bal et al. (1976), with the use of cytochemical techniques, demonstrated that most of the hydrolytic activity was associated with the inner surface of the cell wall. It is already well known that the *LeCel7* expression is auxin-inducible (Wu et al. 1996; Catala et al. 1997). Up-regulation of this enzyme was detected mainly in a rapidly expanding vegetative tissue and in a developing tomato fruit (Catala et al. 1997). Goverse et al. (2000) revealed that auxin-mediated the induction and morphogenesis of a syncytium. In *diageotropica* (*dgt*) tomato mutant – auxin insensitive – the development of a feeding site was significantly inhibited, and only few, half-size females could develop. This reaction was similar to that usually observed on the nematode resistant plants, where only males develop. Karczmarek et al. (2004) observed activation of a DR5 auxin-responsive promoter element 18 h after syncytium induction. It has been suggested that auxin-inducible EGases might be involved in the regulation of cell elongation by generating xyloglucan oligosaccharins (Darvill et al. 1992) or cleaving xyloglucan chains that coated cellulose microfibriles (Rose and Bennett 1999), or even hydrolyzing free ends of newly incorporated xyloglucans (Catala et al. 2000).

Detection of *LeCel8* transcripts and proteins in the 3--day-old syncytia, which might be composed of approximately 100 cells (Sobczak et al. 2005), suggests that this enzyme plays no role in the formation of cell wall openings. However, with the use of the IgY antibodies, we could observe the distribution of the LeCel8 protein only within the syncytial cytoplasm. Immunolabeling patterns, obtained after immunolocalization with the use of chicken antibodies against LeCel7 and LeCel8, were similar for both enzymes. However, in contrast to LeCel7, LeCel8 contains a putative cellulose binding domain (CBD). The biochemical function and substrate specificity can be distinct for enzymes with and without the CBD. It was suggested that the enzymes with CBD can act on glucan chains of cellulose, and xyloglucan coating the cellulose microfibrils (Trainotii et al. 1999). Activity of these enzymes would cause weakening of mechanical properties of the cell wall. Little is known about hormone regulation of the *LeCel8* expression. cDNA of *LeCel8* was isolated from tomato hypocotyls (Catala and Bennett 1998). Other known endoglucanases with CBD were detected during vegetative growth of strawberry fruits and in other green tissues (Trainotti et al. 1999). Our results demonstrated that LeCel8 and LeCel7 were involved in formation of a syncytium. After incorpo-

ration into syncytium, the cells progressively became enlarged. The presence of LeCel7 in the young syncytia suggests its role in extension of the cell wall. Enlargement of the syncytial elements and growing osmotic pressure within syncytia is compensated by thickening of the syncytial wall. The presence of LeCel8 in the 3-day-old syncytia suggests that this enzyme may be involved in thickening of the syncytial wall, but also in its extension. Because antibodies against LeCel8 recognised a fragment of the CBD, we expected its presence in the cell wall. We can only speculate that within syncytia they act on polysaccharides of the cell wall matrix, prior to its deposition into the syncytial wall. It is also possible that LeCel8 proteins, which are localised in the cell wall, are not accessible for antibodies. Although we did not observe LeCel8 proteins in the syncytial wall, we suggest that LeCel8 may be involved in preparing cell wall regions for deposition of cell wall components.

During expansion, the syncytial wall must be strong enough to withstand the internal pressure of growing protoplast, but flexible enough to grow: synthesis, softening and maturation must be co-ordinated. These complex processes of modifications of the cell wall in the developing syncytia require activity of several different types of plant cell wall modifying enzymes. So far not only EGases were detected within syncytia. Pectin methylestherases were found to be up-regulated in and around syncytia and giant cells (Vercauteren et al. 2002). In syncytia induced by soybean cyst nematode (*H. glycines*), expression of polygalacturonase genes was detected (Mahalingam et al. 1999). Genes of α and β expansins are also activated. LeEXP5 is up-regulated in syncytia induced by *G. rostochiensis* in tomato roots (Sobczak et al. 2002). Recently also β expansins, *Sl-EXPB1*, *Sl-EXPB2*, and *SL-EXPA1*, were detected in developing syncytia (Kudla 2006).

Our data confirmed that genes of plant endoglucanases are activated during formation of feeding sites in different host plant-parasitic nematode interaction. Their up-regulation in giant cells (Goellner et al. 2001) as well as in syncytia suggests that *LeCel7* and *LeCel8* may play a role in cell wall modifications that occur during formation of both types of nematode feeding sites, for example during cell wall extension and thickening. We suggest that LeCel7 may be involved in extension of syncytial cell, because of its regular distribution along the inner surface of syncytial wall. Although we did not localize LeCel8 in syncytial wall, based on our observations, we propose that LeCel8 also play a role in syncytial wall rebuilding during cell wall extension or/and thickening.

LITERATURE CITED

ALLAWAY W.G., CARPENTER J.L., ASHFORD A.E. 1985. Amplification of inter-symbiont surface by root epidermal transfer cells in the *Pisonia* mycorrhiza. Protoplasma 128: 227-231.

BAL A.K., VERMA D.P.S., BYRNE H., MACLACHLAN G.A. 1976. Subcellular localization of cellulases in auxin-treated pea. J. Cell Biol., 69: 97-105.

BERRY A.M., McINTYRE L., McCULLY M.E. 1986. Fine structure of root hair infection leading to nodulation in the *Frankia-Alnus* symbiosis. Can. J. Bot. 64: 292-305.

BRUMMELL D.A., HARPSTER M.H. 2001. Cell wall metabolism in fruit softening and quality and its manipulation in transgenic plants. Plant Mol. Biol., 47: 311-340.

CATALA C., ROSE J.K.C., BENNETT A.B. 1997. Auxin regulation and spatial localization of an endo-1,4-β-glucanase and xyloglucan endotransglycosylase in expanding tomato hypocotyls. Plant J., 12: 417-426.

CATALA C., BENNETT A.B. 1998. Cloning and sequence analysis of Tomcel8, a new plant endo-1,4-β-glucanase gene encoding a protein with a putative carbohydrate-binding domain (accession no. AF098292). Plant Physiol. 18: 1535.

CATALA C., ROSE J.K.C., BENNETT A.B. 2000. Auxin-regulated genes encoding cell wall-modifying proteins are expressed during early tomato fruit growth. Plant Physiol., 122: 527-534.

COSGROVE D.J. 2005. Growth of the plant cell wall. Nat. Rev. Mol. Cell Biol., 6: 850-861.

DARVILL A., AUGUR C., BERGMANN C., CARLSON R.W., CHEONG J.-J., EBERHARD S., HAHN M.G., LÓ V.-M. MARFA V., MEYER B., MOHNEN D., O'NEILL M.A., SPIRO M.D., VAN HALBEEK H., YORK W.S., ALBERSHEIM P. 1992. Oligosaccharins-oligosaccharides that regulate growth, development and defence response in plants. Glycobiology, 2: 181-198.

DAVIS E.L., HUSSEY R.S., BAUM T.J. 2004. Getting to the roots of parasitism by nematodes. Trends in Parasitol. 20: 134-141.

DE ALMEIDA ENGLER J., DE GROODT R., VAN MONTAGU M., ENGLER G. 2001. In situ hybridization to mRNA of *Arabidopsis* tissue sections. Methods, 23: 325-334.

DEL CAMPILLO E., BENNETT A.B. 1996. Pedicel breakstrenght and cellulase gene expression during tomato flower abscission. Plant Physiol., 111: 813-820.

ENDO B.Y. 1971. Synthesis of nucleic acids at infection sites of soybean roots parasitized by *Heterodera glycines*. Phytopathology 61: 395-399.

GAO B., ALLEN R., MAIER T., DAVIS E.L., BAUM T.J., HUSSEY R.S. 2004. Molecular characterisation and developmental expression of cellulose-binding protein gene in the soybean cyst nematode *Heterodera glycines*. Int. J. Parasitol., 34: 1377-1383.

GHEYSEN G., FENOLL C. 2002. Gene expression in nematode feeding sites. Ann. Rev. Phytopathol. 40: 191-219.

GOELLNER M., WANG X., DAVIS E.L. 2001. Endo-1,4-β-glucanase expression in compatibile plant-nematode interactions. Plant Cell 13: 2241-2255.

GOLINOWSKI W., GRUNDLER F.M.W., SOBCZAK M. 1996. Changes in the structure of *Arabidopsis thaliana* during female development of the plant parasitic nematode *Heterodera schachtii*. Protoplasma 194: 103-116.

GOLINOWSKI W., SOBCZAK M., KUREK W., GRYMASZEWSKA G. 1997. The structure of syncytia. In: Cellular and molecular aspects of plant-nematode interactions. Kluwer Academic Publishers. 89-97.

GOVERSE A., DE ALMEIDA ENGLER J., VERHEES J., VAN DER KROL S., HELGER J., GHEYSEN G. 2000a. Cell cycle activation by plant parasitic nematodes. Plant Mol. Biol., 43: 747-761.

GOVERSE A., OVERMARS H., ENGELBERTINK J., SCHOTS A., BAKKER J., HELDER J. 2000b. Both induction and morphogenesis of cyst nematode feeding cells are mediated by auxin. Mol. Plant-Microbe Interact., 13: 1121-1129.

GRUNDLER F.M.W., SOBCZAK M., GOLINOWSKI W. 1998. Formation of wall openings in root cells of *Arabidopsis thaliana* following infection by the plant-parasitic nematode *Heterodera schachtii*. Eur. J. Plant Pathol., 104: 545-551.

HENRISSAT B. 1991. A classification of glycosyl hydrolases based on amino acid sequence similarities. Biochem. J. 280: 309-316.

JONES M.G.K., NORTHCOTE D.H. 1972. Nematode-induced syncytium – a multinucleate transfer cell. J. Cell Sci., 10: 787--809.

KARCZMAREK A., OVERMARS H., HELDER J., GOVERSE A. 2004. Feeding cell development by cyst and root-knot nematodes involves a similar early, local and transient activation of a specific auxin-inducible promoter element. Mol. Plant Pathol., 5: 343-346.

KARCZMAREK A. 2006. Dissecting host plant manipulation by cyst and root-knot nematodes. PhD Thesis. University in Wageningen.

KUDŁA U. 2006. The role of cell wall-modifying proteins in plant penetration and feeding site proliferation by the potato cyst nematode *Globodera rostochiensis*. PhD Thesis. University in Wageningen.

LASHBROOK C.C., GONZALES-BOSCH C., BENNETT A.B. 1994. Two divergent endo-1,4-β-glucanases genes exhibit overlapping expression in ripening fruit and abscising flowers. Plant Cell, 6: 1485-1493.

MAHALINGAM R., WANG G., KNAP H.T. 1999. Polygalacturonase and polygalacturonase inhibitor protein: gene isolation and transcription in *Glycine* max-*Heterodera glycines* interactions. Mol. Plant-Microbe Interac., 12: 490-498.

MØLHØJ M., PAGANT S., HOFTE H. 2002. Towards understanding the role of membrane-bound endo-1,4-β-glucanases in celluose biosynthesis. Plant Cell Physiol. 43 (12): 1399--1406.

NIEBEL A., DE ALMEIDA ENGLER J., HEMERLY A., FERREIRA P., INZE D. 1996. Induction of *cdc2a* and *cyc1At* expression in *Arabidopsis* during early phases of nematode-induced feeding cell formation. Plant J. 10: 1037-1043.

OFFLER C.E., MCCURDY D.W., PATRICK J.W., TALBOT M.J. 2003. Transfer cells: Cells Specialized for a Special Purpose. Annu. Rev. Plant Biol. 54: 431-54.

POPEIJUS H., OVERMARS H., JONES J., BLOK V., GOVERSE A., HELDER J., SCHOTS A., BAKKER J., SMANT G. 2000. Degradation of plant cell walls by a nematode. Nature 406: 36-37.

RICE S.L., LEADBEATER B.S.C., STONE A.R. 1985. Changes in cell structure in roots of resistant potatoes parasitized by potato cyst nematodes. I. Potatoes with resistance gene H_1 derived from *Solanum tuberosum* ssp. andigena. Physiol. Plant Pathol. 27: 219-234.

ROSE J.K.C., BENNETT A.B. 1999. Cooperative disassembly of the cellulose-xyloglucan network of plant cell walls: parallels between cell expansion and fruit ripening. Trends in Plant Sci. 4: 176-183.

QIN L., KUDLA U., ROZE E.H.A., GOVERSE A., POPEIJUS H., NIEUWLAND J., OVERMARS H., JONES J.T., SCHOTS A., SMANT G., BAKKER J., HELDER J. 2004. A nematode expansin acting on plants. Nature 427, 30.

SCHEIBE W.-R., PAULY M. 2004. Glycosyltransferases and cell wall biosynthesis: novel players and insight. Curr. Opp. Plant Biol. 7: 285-295.

SMANT G., STOKKERMANS J.P.W.G., YAN Y., DE BOER J.M., BAUM T.J., WANG X., HUSSEY R.S., GOMMERS F.J., HENRISSAT B., DAVIS E.L., HELDER J., SCHOTS A., BAKKER J. 1998. Endogenous cellulases in animals: isolation of β-1,4-endoglucanase genes from two species of plant-parasitic nematodes. Proc. Natl. Acad. Sci. USA. 95: 4906--4911.

SOBCZAK M., AVROVA A., JUPOWICZ J., PHILLIPS M.S., ERNST K., KUMAR A. 2005. Characterization of susceptibility and resistance responses to potato cyst nematode (*Globodera* sp.) infection of tomato lines in the absence and presence of the broad-spectrum nematode resistance *Hero* gene. Mol. Plant-Microbe Interact. 18: 158-168.

SOBCZAK M., FUDALI S., GOLECKI B., JANAKOWSKI S., GRYMASZEWSKA G., KUREK W., LICHOCKA M., GOLINOWSKI W., GRUNDLER F.M.W. 2002. Localisation of expression of Le-Exp5 in feeding sites induced by *Globodera rostochiensis* in roots of susceptible tomato using in-situ RT-PCR method. Nematology 4: 225.

TALBOTT L.D., RAY P.M. 1992. Molecular size and separability features of pea cell wall polysaccharides. Implication for models of primary wall structure. Plant Physiol. 92: 357-368.

TRAINOTTI L., SPOLAORE S., PAVANELLO A., BALDAN B., CASADORO G. 1999. A novel E-type endo-β-1,4-glucanase with a putative cellulose-binding domain is highly expressed in ripening strawberry fruits. Plant Mol. Biol. 40: 323-332.

VERCAUTEREN I., DE ALMEIDA ENGLER J., DE GROODT R., GHEYSEN G. 2002. An *Arabidopsis thaliana* pectin acetylesterase gene is upregulated in nematode feeding sites induced by root-knot and cyst nematodes. Mol. Plant-Microbe Interact. 15: 404-407.

WU S.-C., BLUMER J.M., DARVILL A.G., ALBERSHEIM P. 1996. Characterization of an endo-β-1,4-glucanase gene induced by auxin in elongating pea epicotyls. Plant Physiol., 110: 163-170.